J Mater Sci (2011) 46:3693–3697
DOI 10.1007/s10853-010-5123-y

Synthesis and characterization of vanadium carbide nanoparticles by thermal refluxing-derived precursors

Fei Liu · Yadong Yao · Hao Zhang ·
Yunqing Kang · Guangfu Yin · Zhongbing Huang ·
Xiaoming Liao · Xiaofeng Liang

Received: 28 August 2010 / Accepted: 29 November 2010 / Published online: 12 February 2011

Abstract Vanadium carbide (VC) nanoparticles were synthesized by a novel refluxing-derived precursor. The organic/inorganic hybrid precursor was prepared by a two-step refluxing method using hydrous V_2O_5 as vanadium source and *n*-dodecane as carbon source. The reaction process, phase composition, microstructure, and element composition of VC were investigated by X-ray diffraction (XRD), Raman spectroscopy, scanning electron microscopy, and X-ray photoelectron spectroscopy (XPS). The results showed that VC nanoparticles could be obtained at 900 °C for 1 h in flowing Argon (Ar), which was much lower than those of conventional synthesis methods. XRD pattern indicated that the product was face-centered cubic VC with a lattice constant $a = 4.1626$ Å and average crystallite size of 22.3 nm. Raman spectra indicated that long time refluxing resulted in alkane dehydrogenation and the formation of coke on V_2O_5 nanoparticles. XPS investigations confirmed oxygen presence in VC lattice. Electron microscopy photographs showed the particle size ranged from 20 to 50 nm. All these results confirmed that the two-step refluxing method was a novel and feasible method to synthesize VC nanoparticles.

Introduction

The transition metal carbides have been widely used in metallurgy, electronics, catalysts, and high temperature covering materials [1–3] due to their high melting points, high hardness, high temperature strength, and good electrical and thermal conductivities [4–6].

Currently vanadium carbide powders have been synthesized by various methods, including direct element reaction [7], mechanical alloying [8], temperature-programmed reaction [9–12], and gas reduction–carburization [13–16]. However, industrial applications of the methods are still limited due to the agglomeration problems [7], wide size distributions [7], low yields [7, 8], complex monitoring [9–12], and high costs [13–16].

Some transition metal oxides such as supported vanadia (VO_x) catalysts have been found to be the most reactive catalysts in a number of catalytic reactions including direct dehydrogenation of alkanes [17–19], but the deactivation due to the build-up of surface carbonaceous residues is still a problem. The highly carbonaceous or coke species still exist after the combustion [20]. Inspired by the catalyst deactivation due to carbon deposition, a novel method of synthesizing VC nanoparticles by a novel precursor was reported. The precursor was synthesized by a two-step refluxing method using hydrous V_2O_5 and *n*-dodecane as raw materials.

The refluxing technique has a number of potential advantages: (1) it has been seldom reported in the literature, (2) a close contacts of the reactants can be achieved, (3) the VC nanoparticles can be obtained at a lower temperature which is much lower than those of conventional synthesis methods [7–16], and (4) the carbon content in refluxing-derived precursor can be controlled by the refluxing time and the *n*-dodecane can be reused. This

---

F. Liu · Y. Yao (✉) · H. Zhang · Y. Kang · G. Yin ·
Z. Huang · X. Liao · X. Liang
College of Materials Science and Engineering, Sichuan
University, Chengdu 610064, People's Republic of China
e-mail: yaoyd426@yahoo.com.cn

X. Liang
Analytical and Testing Center,
Southwest University of Science and Technology,
Mianyang 621010, People's Republic of China

study provides a reference and attempt to synthesize vanadium carbide nanoparticles at milder conditions.

Experimental

In a typical experiment, 15 g ammonium vanadate (NH_4VO_3, purity >99%) was heated at 800 °C for 0.5 h and then was quickly put into the distilled water with high-speed stirring. The certain amount of diluted ammonia was added into the system and its pH value was controlled to 7–8 to form hydrous V_2O_5 precipitations. First, a suspension consisted of the hydrous V_2O_5 precipitations and 400 mL ethanol was refluxed at 70 °C for 1 h and the refluxing process was repeated five times to remove the integrated water in hydrous V_2O_5. Second, the obtained precipitations were re-dispersed in 400 mL *n*-dodecane, refluxed at 210 °C for 1, 2, 3, and 4 days. The prepared precursors were labeled as RA1, RA2, RA3, and RA4, and the precursor without being refluxed was labeled as RA. Finally, the refluxing-derived precursors were obtained by drying the precipitation at 120 °C for 2 h. The VC nanopowders could be prepared by thermal processing the precursors in vacuum or in a high purity Ar atmosphere.

The structure of the nanoparticles was examined at room temperature via a DX-1000 diffractometer using Cu-Kα radiation in the range of $2\theta = 20$–80° with a scanning rate of 3.6° (2θ) per minute. The average crystallite size of the nanoparticles was calculated based on XRD peak broadening using the Scherrer formula.

$$D = k\lambda/\beta\cos\theta. \quad (1)$$

In Eq. 1 D represents the average crystallite size; the constant k is 0.9; λ is the wave length of the X-ray radiation; β is the broadening of the diffraction line measured at half maximum intensity, and θ represents the Bragg angle. The correction for instrumental broadening was taken into account in the measurement of the peak broadening. Raman data were collected on a Renishaw InVia microRaman system and fitted using a non-linear least squares fit with a Gaussian peak shape. The X-ray photoelectron spectroscopy (XPS) was carried out using a XSAM 800 spectrometer (Kratos, England) using the Mg-Kα X-ray source. Scanning electron microscopy (SEM) images were obtained on a Hitachi S-4800 electron microscope.

Results and discussion

In order to determine the content of the precursors, we heated the dried precursors at 700 °C for 1 h in air then the weight loss before and after calcination could be calculated as the C content of the precursors, which is showed in Table 1.

It is seen that the weight loss of the precursor RA without being refluxed is 2.1 wt% which can be ascribed to the water and air absorbed on the surface. The C content of the precursors being refluxed increased with the refluxing time added. We can also control the C content of the precursor by changing the refluxing time. The C content of RA4 is 46.6 wt%, which is much more than 31.3 wt% required theoretically in the carbothermal reduction reaction:

$$V_2O_5(s) + 7C(s) = 2VC(s) + 5CO(g). \quad (2)$$

In order to know the the C content of the precursor accurately, CH microanalyses were carried out to check the carbon content of RA3. The result shows the carbon percentage, hydrogen percentage, and C:H ratio in the precursor are 36.8, 3.24 wt%, and 0.95, respectively. The C:H ratio of the refluxed-derived precursor was found to be 0.95:1, which is much more than that of saturated *n*-dodecane (0.462:1). It indicates that dehydrogenation of alkane takes place and new highly carbonaceous unsaturated organic substance forms during the refluxing.

Figure 1 gives a comparison of Raman spectra of pure *n*-dodecane and the precursors (consisted of V_2O_5 and highly carbonaceous carbon species). The Raman spectra for *n*-dodecane and the precursors were recorded in spectral regions (1000–3500 cm^{-1}). Figure 1a shows spectra in the C–C stretching and C–H deformation region of *n*-dodecane. It can be seen that several Raman bands appear at 1075, 1300, 1450, 2725, and 2889 cm^{-1}. The band at 1075 cm^{-1} is assigned to the C–C stretching vibration, and the band at 1300 and 1450 cm^{-1} is a deformation mode of the CH_2 and CH_3 group. The two bands at 2725 and 2889 cm^{-1} can be attributed to symmetric and asymmetric stretching vibrations of the CH_2 and CH_3 group [20, 21]. Typical Raman spectra of surface carbon species on the precursor are shown in Fig. 1b. It shows that the CH characteristic peaks at 2725 and 2889 cm^{-1} disappeared, indicating that the alkane carbon chains were dehydrogenated during refluxing. Typical Raman spectra in the regions 1000–2000 cm^{-1} are shown in the inset using a non-linear least squares fit with a Gaussian peak shape.

Table 1 Element content of the precursor (V, O, C)

Samples	V, O (wt%)	C (wt%)
RA	97.9	2.1
RA1	75.3	24.7
RA2	62.9	37.1
RA3	58.7	41.3
RA4	53.4	46.6

Two peaks at 1414 and 1586 cm^{-1} during dehydrogenation can be assigned to the formation of coke [21–23]. It is generally accepted that deposition of coke occurs through dehydrogenation, condensation, polymerization, and cyclisation of hydrogen deficient hydrocarbon species on the surface of the catalyst and the coke are mostly olefins and aromatics [22]. In this article, the V_2O_5 catalytic behavior results in the dehydrogenation during long time refluxing.

In order to determine the phase composition and the crystal structure of the synthesized samples, X-ray diffraction measurement was carried out on the samples. Figure 2 shows the XRD patterns of the precursor RA3 being heat treated in Ar at 800–1200 °C for 1 h. From Fig. 2a, it can be seen that all peaks obtained at 800 °C can be indexed as V_2O_3 (JCPDS 34-0187) which belongs to the close-packed hexagonal structure with the lattice parameters $a = 4.954$ Å and $c = 14.008$ Å except for a little of amorphous carbon. The pattern of the sample obtained at 900 °C (shown in Fig. 2b) consists of peaks corresponding to V_2O_3 (JCPDS 34-0187) and VC (JCPDS 73-0476) which belongs to the cubic structure with the lattice parameters $a = 4.165$ Å. This indicates that the oxidation–reduction reaction between V_2O_3 and amorphous carbon could occur at 900 °C. When the temperature rises to 1200 °C, its diffraction curve as shown in Fig. 2e can be indexed as cubic VC (JCPDS 73-0476) and no obvious evidences of impurities such as vanadium oxides and other vanadium carbides can be found in this XRD pattern. This indicates that V_2O_3 can thoroughly transform into VC in 1200 °C. The crystallite size (Fig. 2e) as calculated from the Scherrer equation is 22.3 nm. The refinement gives the cell constants, $a = 4.1626$ Å (Fig. 2e), which is consistent with the value reported in the literature ($a = 4.165$ Å) (JCPDS card No. 73-0476).

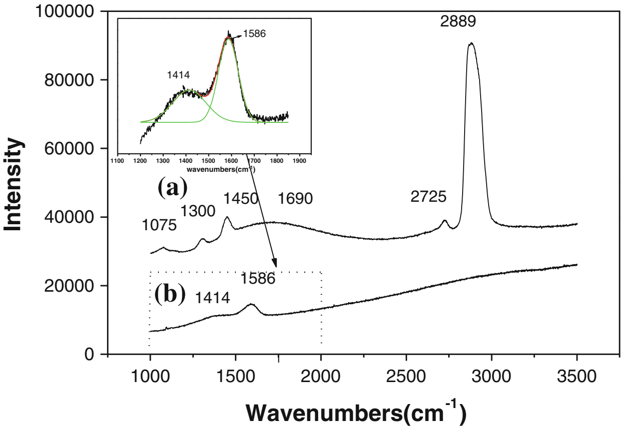

Fig. 1 Raman spectra of (*a*) *n*-dodecane and (*b*) RA3, the *inset* of a local magnified and Gauss function fitting pattern from the *dotted area*

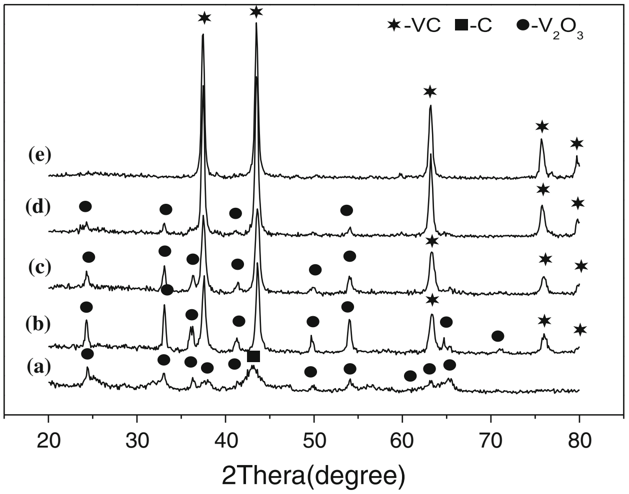

Fig. 2 XRD patterns for the samples obtained from the precursor RA3 at: (*a*) 800, (*b*) 900, (*c*) 1000, (*d*) 1100, and (*e*) 1200 °C for 1 h

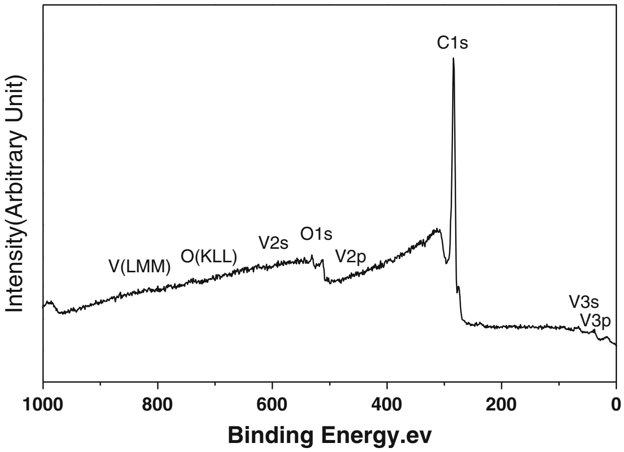

Fig. 3 XPS spectra of product obtained from the precursor RA3 at 1200 °C for 1 h

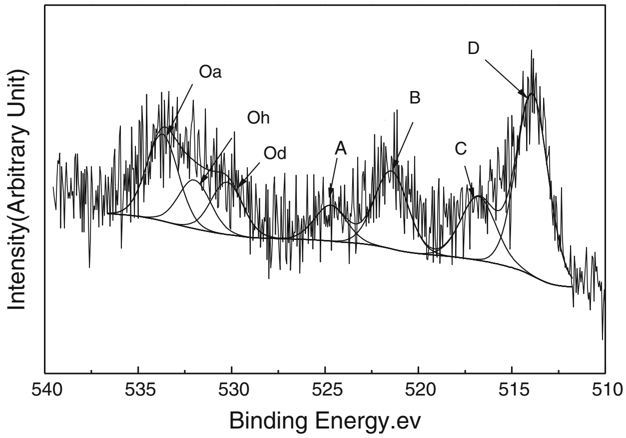

Fig. 4 XPS spectrum of O1*s* and V2*p* energy region for the sample obtained from the precursor RA3 at 1200 °C for 1 h

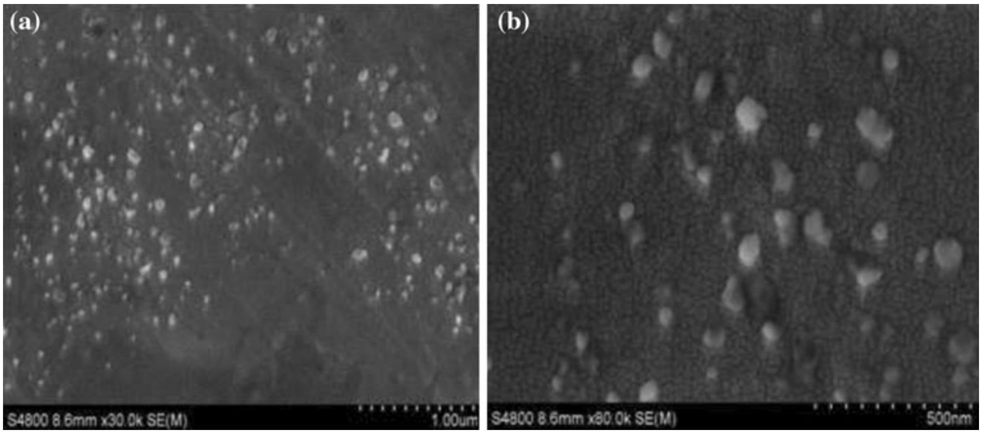

Fig. 5 SEM photographs of the sample obtained from the precursor RA3 at 1200 °C for 1 h

In order to determine the element composition and binding state, simultaneous XPS was carried out on the sample obtained from the precursor RA3 at 1200 °C for 1 h as shown in Fig. 3. From Fig. 3, it can be seen that the surface of the specimen mainly consists of V, C, and O three species elements. The peak size of O1*s* between 528.0 and 536.0 eV is fairly large and the spectrum of O1*s* is not symmetric. The XPS spectrum of O1*s* and V2*p* energy region for vanadium carbide obtained from the precursor RA3 at 1200 °C for 1 h is shown in Fig. 4. The peaks of Oa (533.7 eV) and Oh (532.0 eV) should result from O^- and OH^-, respectively [24, 25]. Two oxygen peaks mainly originated from air, which can be removed by drying the sample at certain temperature. The O1*s* peak with the binding energy of Od (530.3 eV) is ascribed to vanadium dioxide (V^{4+}) [25]. The peaks of A (524.7 eV) and C (516.8 eV) should result from V2*p*1/2 and V2*p*3/2 spin–orbit components of VO_2, respectively. The peaks of B (521.5 eV) and D (513.9 eV) can be ascribed to V2*p*1/2 and V2*p*3/2 spin–orbit component of VC, respectively [26]. The results agree well with the XPS spectrum of O1*s* energy region for vanadium carbide as shown in Fig. 4. However, this vanadium oxide does not appear in the XRD pattern (Fig. 2e), showing that the content of the vanadium oxide is very little.

Figure 5 shows typical SEM micrographs of the sample obtained from the precursor RA3 at 1200 °C for 1 h. It is shown that the VC nanoparticles had a very fine particle size in the SEM image. The particles obtained show good performance of crystallization and dispersity and they are mainly composed of uniformly sized spherical particles. In this image, the sample shows that it consists of particles in the range of 20–50 nm in diameter which is in accordance with that of the calculated result from the XRD pattern.

Conclusions

Here, we report a method of thermal processing the precursor to synthesize vanadium carbide nanoparticles. The precursor was prepared by a feasible two-step refluxing method using hydrous V_2O_5 as vanadium source and *n*-dodecane as carbon source. XRD results show that the single phase VC powders can be prepared at ~1200 °C for 1 h with the average crystallite size of 22.3 nm. SEM results show that the nanoparticles have good performance of crystallization and dispersity. The technique provides a reference and attempt to synthesize vanadium carbide nanoparticles at milder conditions.

Acknowledgements The support of Sichuan Province through a Key Technologies Research and Development Program of Sichuan Province, the New Preparative Technique of Nano Carbides (2006Z02-17) is acknowledged with gratitude. We thank Southwest University of Science and Technology for providing the Raman spectra tests.

References

1. Reichl W, Hayek K (2004) J Catal 222:53
2. Yazawa Y, Furuhara T, Maki T (2004) Acta Mater 52:3727
3. Wiesenberger H, Lengauer W, Ettmayer P (1998) Acta Mater 46:651
4. Misra RDK (1996) Acta Mater 44:4367
5. Lee J, Sohn K, Hyeon T (2001) J Am Chem Soc 123:5146
6. Yoon SB, Sohn K, Kim JY, Shin CH, Yu JS, Hyeon T (2002) Adv Mater 14:19
7. Zhang B, Li ZQ (2005) J Alloys Compd 392:183
8. Zhang B, Li ZQ (2005) J Alloys Compd 392:183
9. Kapoor R, Oyama ST (1995) J Solid State Chem 120:320
10. Lee JS, Oyama ST, Boudart M (1987) J Catal 106:125
11. Ribeiro FH, Dalla Betta RA, Boudart M, Baumgartner J, Iglesia E (1991) J Catal 130:86
12. Iglesia E, Baumgartner J, Ribeiro FH, Boudart M (1991) J Catal 131:523
13. Neylon MK, Choi S, Kwon H, Curry KE, Thompson LT (1999) Appl Catal A Gen 183:253
14. Lee JS, Locatelli S, Oyama ST, Boudart M (1990) J Catal 125:157
15. Oyama ST, Schlatter JC, Metcalfe JE III, Lambert JM (1988) Ind Eng Chem Res 27:1639
16. Lee JS, Volpe L, Ribeiro FH, Boudart M (1988) J Catal 112:44
17. Lemonidou AA (2001) Appl Catal A Gen 216:277
18. Lopez Nieto JM, Concepcion P, Dejoz A et al (2000) J Catal 189:147

19. Wachs IE, Weckhuysen BM (1997) Appl Catal A Gen 157:67
20. Li J, Xiong G, Feng Z et al (2000) Microporous Mesoporous Mater 39:275
21. Atamas NA, Yaremko AM, Seeger T et al (1997) J Mol Struct 708:189
22. Chua YT, Stair PC (2003) J Catal 213:39
23. Veres M, Fule M, Toth S, Koos M, Pocsik I (2004) Diamond Relat Mater 13:1412
24. Liao SJ, Huang DG, Yu DH (2004) J Photochem Photobiol A Chem 168:7
25. Ye JW, Liu Y, Zhao ZW, Jiang ZT, Tang ZH (2010) J Alloys Compd 496:278
26. Choi JG (1999) Appl Surf Sci 148:64